Muography for Underground Geological Surveys: Ongoing Application at the Lousal Mine (Iberian Pyrite Belt, Portugal)

P. Teixeira,[1] L. Afonso,[2] S. Andringa,[2] P. Assis,[2,3] M. Bezzeghoud,[1] A. Blanco,[2] J. F. Borges,[1] B. Caldeira,[1] L. Cazon,[2] P. Dobrilla,[2] L. Lopes,[2] J. X. Matos,[4] R. J. Oliveira,[1] M. Pimenta,[2,3] R. Sarmento,[2] and B. Tomé[2]

[1]*Physics Department (ECT), Institute of Earth Sciences (ICT/IIFA), Earth Remote Sensing Laboratory (EaRSLab), University of Évora, Rua Romão Ramalho no. 59 7000-671 Évora, Portugal*

[2]*Laboratory of Instrumentation and Experimental Particle Physics (LIP), Av. Prof. Gama Pinto, 2 1649-003 Lisboa, Portugal*

[3]*Instituto Superior Técnico (IST), Av. Rovisco Pais, 1, 1049-001 Lisboa, Portugal*

[4]*Laboratório Nacional de Energia e Geologia (LNEG), Campus de Aljustrel, Bairro da Vale d'Oca, Apartado 14, 7601-909 Aljustrel, Portugal*

Corresponding author: P. Teixeira
Email: pmmt@uevora.pt

Abstract

The use of muons for geophysical surveys has been proved successful in numerous projects around the planet. The use of muography in an underground environment has an easy side, when compared to the surface, due to the absence of the background radiation. On the other hand, the muon flux is much lower than what is measured on the surface. Geological and underground conditions should be considered when defining the required exposure time and developing suitable muon telescopes for the observation. A collaboration has been established between the Institute of Earth Sciences (ICT), University of Évora, the Laboratory of Instrumentation and Experimental Particle Physics (LIP), and the Lousal Ciência Viva Center to develop muon detectors and evaluate the muography potential in the Lousal Mine, with the general aim to create the conditions to use muography as a novel method for geophysical surveys in Portugal. The Lousal Mine (Iberian Pyrite Belt) was exploited until 1988 and is presently an excellent European example of environmental rehabilitation and social improvement based on museum, scientific, and educational activities. The observations are done from the Waldemar mine gallery, about 18 m below the surface. The telescopes, developed by LIP, use robust RPC detectors to observe the crossing muons in real time. The aim is to do a first geological survey of the region with muography, mapping already known structures and ore lenses and measuring their densities. The new data will then be used to improve the existing information, but the full process also serves to test the performance of the muon telescope and of the muography analysis tools. A reference 3D model is being created by joining pre-existing geological and geophysical information and new measurements, done, namely, with seismic refraction and Ground Penetrating Radar (GPR). This model provides a reference against which to compare the muography results. Ideally, muography could be used to produce an equivalent 3D map of densities. This reference 3D model constructed with independent methods will be used to cross-check the muography results.

Keywords: underground muography, geophysical survey, Lousal Mine, Iberian Pyrite Belt
DOI: 10.31526/JAIS.2022.287

1. INTRODUCTION

Muography is a probing technique that relies on atmospheric muons, elementary particles present in particle showers created by cosmic rays when hitting the molecules of the Earth's atmosphere. For it to work, we need muon detectors assembled in a structure that is called a muon telescope, because they measure muon directions.

Both muon scattering and muon transmission can be used, depending on the purpose or scale of the observation. Two muon telescopes, placed around a small- or medium-scale target, can be used to measure the multiple Coulomb scattering effects caused by high-Z nuclei—allowing for quick detection of those materials. One single telescope can be used to measure the muons that are transmitted in each direction, according to the total matter depth crossed in each direction, across larger targets and longer time exposures. Both techniques produce images called muographs that give us information about the density distribution of materials crossed by the muons.

Muography has been applied in different fields, like geosciences, archaeology, civil engineering, cargo surveillance, and nuclear reactor and waste control. There are already well-written reviews about the principles of muography, muon detectors, and some of its applications [1, 2, 3]. This paper aims to share the work done so far in one more study within geosciences, which is using transmission muography.

The use of muography for underground geological surveys has been the aim of the Lousal Muography Project (LouMu) [4], which is now applying it to the Lousal Mine, located in Portugal, in the Iberian Pyrite Belt mineral province. The work is in an early phase, but the goal is to develop and make muography available in Portugal for applications in geophysics. It is a collaboration between the following partner institutions: the Laboratory of Instrumentation and Experimental Particle Physics (LIP), the Institute of Earth Sciences of the University of Évora (ICT-UE), the Lousal Ciência Viva Center (science museum), and Laboratório Nacional de Energia e Geologia (LNEG). The main work is divided into the creation of simulations and development of muography analysis tools, geological and geophysical work to study the land above the mine, and the development of muon telescopes and the application of muon tomography in the Lousal Mine.

The LouMu team is comprised of three multidisciplinary groups: the Particle Physics and Instrumentation Group (members of LIP), the Geophysics and Geology Group (members of ICT-UE and LNEG), and the Outreach Only Team (members of the Lousal Ciência Viva museum). A webpage containing information about the project and the different aspects of the work was created and is publicly available [5].

The Lousal Mine is located on the outskirts of the science museum, and its integration in the public tours offers a great opportunity for education and outreach activities that represent a major aspect of the project. The three collaborating groups are involved and contribute to this task, with outreach activities being done in the science museum, schools, and universities [6].

2. MUOGRAPHY AT THE LOUSAL MINE

The Lousal Mine is located in the NW region of the Iberian Pyrite Belt, a volcanic-hosted massive sulfide (VHMS) deposit province. The first muography tests are done in the southern sector of the mine, profiting from the existence of an old mine gallery named Waldemar, presently with excellent access conditions. The mine operated between 1900 and 1988 for the extraction of massive sulfides. After it was closed, it was requalified and transformed into a science museum that is integrated into the network of national Ciência Viva (Living Science) museums [7]. The geology of the mine gallery is dominated by the Volcano-Sedimentary Complex (VSC) black shales (Late Famennian age and mineralization host rocks) and by the Phyllite-Quartzite Group (PQG) phyllites and quartzites (from the Famennian age), which are present in a narrow and near-vertical antiform [8, 9, 10]. The geological setting, coupled with the infrastructures provided by the museum, makes this an ideal location to test the muography in an underground environment. The Waldemar Gallery is the uppermost gallery of the mine, and it is where this muography study is taking place. The mine tunnel is horizontal and easy to cross. Its entrance is at surface level, but the rest of the tunnel has land above it, specifically between 12 m and 18 m depth. In the central sector of the gallery, there is a vertical access shaft, named the Waldemar Shaft.

The goal of the project is to map the densities between the surface and the gallery, in order to evaluate the performance of the detectors and the muography analysis methods by comparing them with existing information, and later on improve the existing knowledge with the new measurements provided by muography.

The different observation positions were chosen, taking into account space availability and also the local geology, by choosing some geological features as the main targets for observation. These targets are shown in Figure 1. A subvertical regional geological fault (the Corona Fault) in the north-northeast (NNE) direction crosses one of the observation regions (Figure 1(a)). The rocks in the fault region have lower compaction, due to the fault movement, which translates into a lower average density. In addition, the mine has an iron caprock above the gallery, which is an intensely oxidized and weathered rock deposit with mainly iron oxides in its constitution, and other mineralizations of iron-rich sedimentary rocks, visible in the gallery walls (Figures 1(c) and 1(d)). Both have higher average densities than the host rock.

3. RPCS AND MUON TELESCOPES

The muon telescopes built within the LouMu collaboration are equipped with Resistive Plate Chambers (RPCs). RPCs are a type of gaseous particle detectors, used to track charged particles. The passage of muons ionizes the gas and causes an avalanche of electrons that produce an electrical signal. The trajectory of the muons is given by simultaneous detection in the different parallel RPCs. The gas is sent to the RPCs and collected with a low flux, from a container outside the mine, without leakage to the environment.

The detector laboratory at LIP developed RPCs that are robust and can work reliably and autonomously for muon detection at the Pierre Auger Observatory [11, 12]. The LouMu telescope used the same kind of RPC planes and electronics readout.

The operation parameters (e.g., applied high-voltage) can be adapted according to the temperature and humidity of the environment; combined with low gas and electricity consumption and low maintenance needs, these make them ideal for use in remote and outdoor environments [13]. The telescope is made of several RPC planes, and data is taken when two of them have coincident signals; RPCs good time and position resolution make them also suitable for muon tracking in real time and high angular resolution. An Internet connection to the muon telescope enables the muography data analysis to be made while the observation is taking place.

In 2019, a prototype was installed inside the gallery to test the equipment's response to the mine environment. It is equipped with 2 square-shaped RPCs measuring 30 centimeters side and assembled with the necessary electronic and gas components (Figure 2(a)). Each detector has a resolution of only 3 by 3 pixels, and the small telescope was mostly used to test the working conditions. After the test period ended, it became a demonstrator inside the mine for outreach activities within the museum tours.

A fully functioning and bigger muon telescope, nicknamed "CorePix", was built after the MiniMu test phase and is currently in the LIP detectors laboratory collecting data for calibration purposes. It is assembled with 4 RPC detectors with 64 channels each, with a detection area of 1 m $\times$ 1 m (Figure 2(b)). Inside the RPCs, the detection pads are configured in different shapes, and three

(a) (b)

(c) (d)

FIGURE 1: Geological targets for the muography observations: (a) Corona Fault; (b) Lousal mine iron caprock; (c) massive sulfides oxidized; (d) iron-rich black shale.

(a) (b)

FIGURE 2: (a) MiniMu prototype used to test the equipment and dissemination of the project inside the Lousal mine gallery (the gas container on the right of the MiniMu was later placed in a storage room, outside the mine, at the entrance; (b) CorePix muon telescope with four RPCs during the optimization phase in the LIP detectors laboratory.

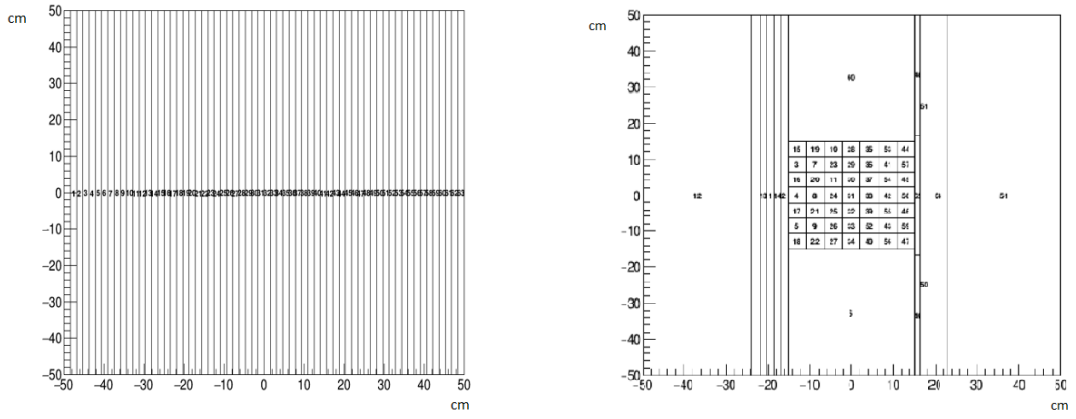

(a) (b)

FIGURE 3: Configuration of the 64 pads in the RPCs. In the CorePix telescope, the upper RPC has the pads arranged in columns (a). The other 3 RPCs have the pads configured as shown in (b) with the center (the CorePix) divided into smaller pads for higher resolution.

of the planes have a higher resolution in the center, the CorePix (Figure 3). The observation resolution can be adjusted by moving the RPC planes along the structure and changing the distance between the planes accordingly.

In the laboratory, it has been collecting data in different positions and creating muographs of the building above it. Simulated muographs of the same conditions are also created for comparison [6]. The purpose of this test phase is to evaluate and correct, when necessary, the pads, detection uniformity and efficiency, before the telescope is moved to the Lousal Mine.

4. GEANT4 SIMULATIONS

While the CorePix is not ready to be installed in the mine, the simulation and analysis tools necessary for the interpretation of the muography observations are also being prepared.

The Geant4 [14, 15] toolkit is used to simulate the passage of atmospheric muons through simplified geometries representing several scenarios in the mine. These simulations are an essential part of muography work, to study the muon attenuation and to use as references in the muographic data analysis. The atmospheric muon flux at sea level is used as input to the simulation. The parameterization given in PDG2010 [16], as a function of muon energy and zenith angle, is used. The expected numbers for muons arriving per unit area and time are calculated by integrating the flux in energy and solid angle. The reference value obtained at the surface is 250 muons/m^2/s, and the value drops to 30 muons/m^2/s around the gallery level; i.e., the transmission down to the gallery is only 12%.

In the Geant4, muons are injected inside the simulation volume, built with a geometry thought for analyzing ground structures, densities, and other parameters of the observation. In this case, the injection area is the surface of the ground volume ($60 \times 60\,m^2$), and the injected muon flux has an energy cut calculated for the detector depth. Only the muons whose direction is expected to reach the $1\,m^2$ detector area (or an area around it, considering the Coulomb dispersion that can occur in the muons interactions while crossing the ground) are tracked in the simulation.

Simulations were used to study the exposure needed to identify a small 1 m radius spherical volume, 10 m above the detector, inside the ground volume (Figure 4).

The host rock volume is made of a homogeneous chemical compound equivalent to shale (density $2.6\,g/cm^3$). The ground volume is 20 m deep, and the detector is placed at the bottom. Different mineralogical compositions which correspond to different densities of the spherical body were tested, and the exposure time needed to distinguish the ore sphere from the host rock was taken from the muographs analysis.

In the analysis of the simulation muographs, the ratio (equation (1)) and the significance (equation (2)) are the quantitative parameters that are used to enhance the density differences.

$$\text{Ratio} = \frac{N_{\text{sphere}}}{N_{\text{reference}}}, \tag{1}$$

$$\text{Significance} = \frac{\left(N_{\text{sphere}} - N_{\text{reference}}\right)}{\left(\sqrt{N_{\text{sphere}}{}^2} + \sqrt{N_{\text{reference}}{}^2}\right)^{\frac{1}{2}}}, \tag{2}$$

where N_{sphere} are the muon counts in the presence of the sphere and $N_{\text{reference}}$ are the muon counts in the absence of the sphere. The denominator of equation (2) is the statistical uncertainty associated with the muon counts in the $1\,m \times 1\,m$ detector and is used

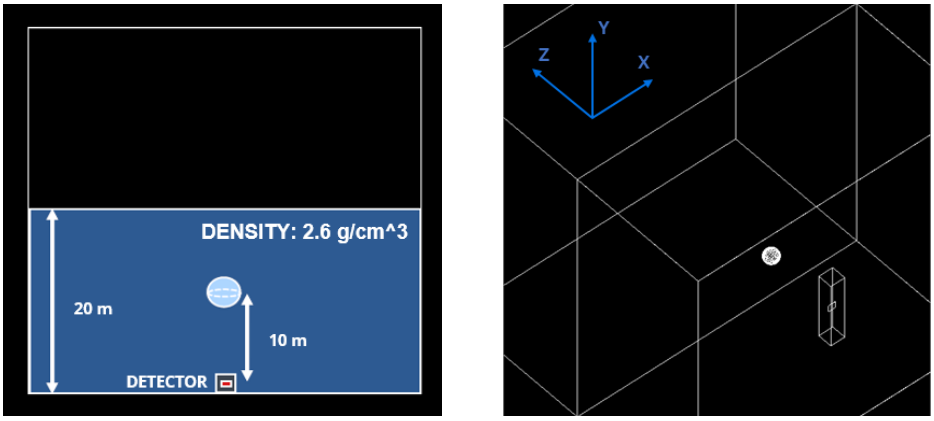

(a) (b)

FIGURE 4: Simple geometry based on the mine scenario with a sphere inside a volume of rock to test the identification of different ore minerals: (a) side view; (b) 3D view.

to take into account the statistical fluctuation in muon counts, so that the real density contrasts become clearer. In the muograph analysis, significance above 5 sigma of statistical uncertainty is considered clear identifications of the spherical body.

The results for a 1 day $\times$ 1 m^2 exposure comparing the presence or absence of a sphere of air can be viewed in 1D or 2D histograms (Figures 5(a) and 5(b)), which show that 10% more muons arrive vertically to the detector when crossing the sphere and that a large significance can be obtained in just 1 day. The sphere is visible in the 1D ratio histogram as the leftmost red dot, with a ratio value significantly above the line of value 1 (meaning higher muon counts detected compared to the reference) and in the 2D histogram as the darker red center pixel, denoting 10% more muon counts from the vertical direction. In the 2D significance histogram, the statistical fluctuations visible in the 2D ratio histogram are gone, and the presence of the sphere is clear. It is visible as the bright red center pixel; the color indicates a value of 5 sigma or above, which denotes a certainty of different densities. In the 1D significance histogram, from the direction of the sphere (leftmost column, vertical direction), the significance calculated is above 60 sigma.

Keeping the other conditions fixed in the simulation, and changing the density of the sphere and/or the exposure time, we obtain general expressions that can be used to extrapolate this result still within this ideal scenario (Figures 5(c) and 5(d)). Within the range considered, the attenuation depends linearly on the density difference between the sphere and the surrounding material, increasing by $\sim$2% as the density is increased by 1 g/cm^3. Large differences of 3 g/cm^3 could be observed in much shorter times below the scale of days, while an infinite time is needed if the sphere has the same density as the surrounding. The attenuation linear equation (Figure 5(c)) gives ratio (R) as a function of density difference (x). Using the R equation, the expected attenuation for materials with other density differences can be calculated. The exponential equation (Figure 5(d)) gives the exposure time (ET, in days) at 5-sigma significance as a function of density difference (x). Using the ET equation, the exposure time at 5 sigma for materials with other density differences can be calculated. Considering the density difference between the air sphere (density $\sim$0 g/cm^2) and the host rock (density 2.6 g/cm^2), the ET, in this case, is less than 1 day.

The latest approach in the simulation studies used a more realistic geometry of the Waldemar Gallery, which is crossed by a regional fault zone that has a mean density lower than the host rock (fault density in the simulation: 2.2 g/cm^3). This simulation geometry also includes the mine shaft that connects the surface to the gallery level (Figures 6(a), 6(b), and 6(c)). The fault is the test target in this simulation, with a 0.4 g/cm^3 density value lower than the host rock volume, which has a density of 2.6 g/cm^3.

The existence of the fault zone changes the symmetry of the muon counts (Figure 6(e)), when compared to the muograph without the fault, with only the shaft visible as the red spot (Figure 6(d)). Because the fault zone has a lower density than the host rock, more muons will arrive at the detector from its direction. The muographs correspond to an exposure time of 4 days and to an observation area of about 30 by 30 m at the surface level.

Repeating the analysis of the ratio and significance parameters, but now using as a reference the same geometry but without the fault volume, only the differences between this and the full model remain, and the presence of the fault stands out (Figures 6(f) and 6(g)). In the ratio 2D histogram (Figure 6(f)), the fault is visible in light red, indicating that the muon detection increased by about 10%. In the significance 2D histogram (Figure 6(g)), the fault is visible in bright red, indicating that the value is 5 sigma or above.

It is important to build good references for the analysis so that already known features can be taken into account, and the analysis can be concentrated on the targets to be studied and on unknown ones that can appear in real observations.

5. GEOLOGICAL AND GEOPHYSICAL SURVEY

To evaluate and compare the muography data to the geological information, there is a benefit in knowing the surface and the ground above the telescope location in depth. Geological and geophysical surveys have been and will be carried out further us-

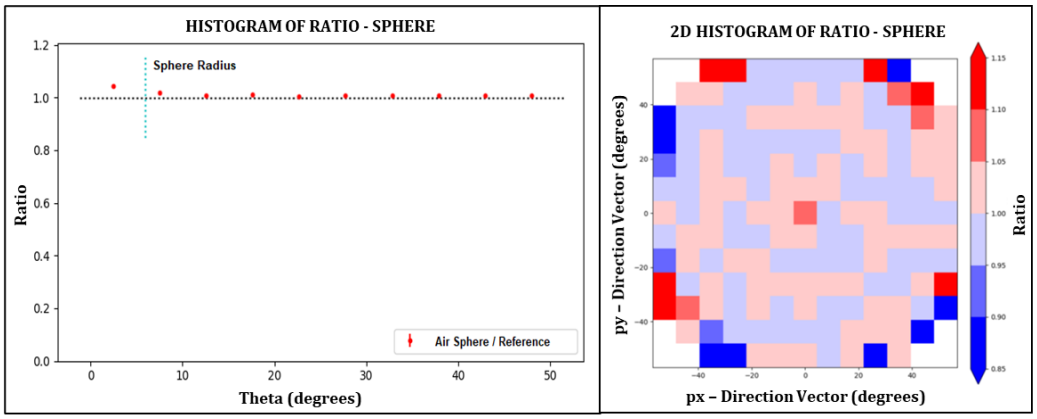

(a)

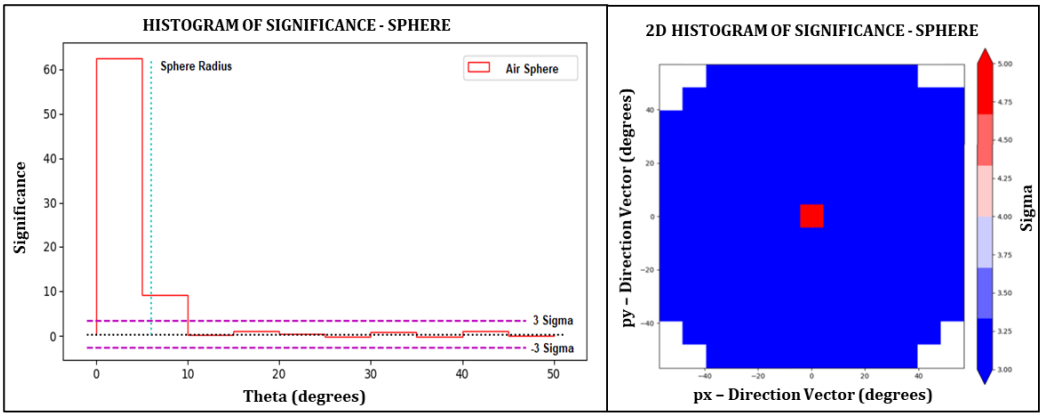

(b)

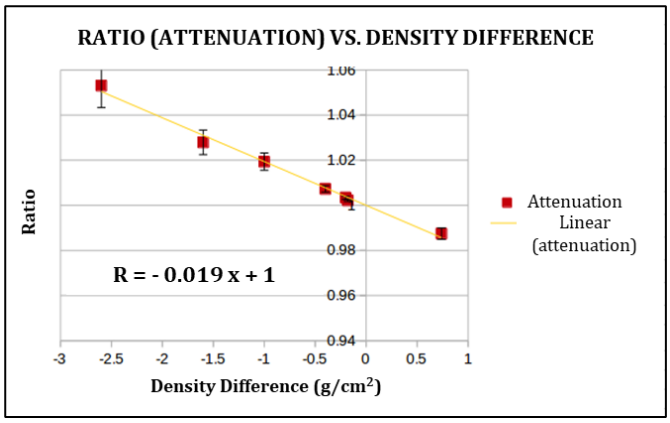

(c)

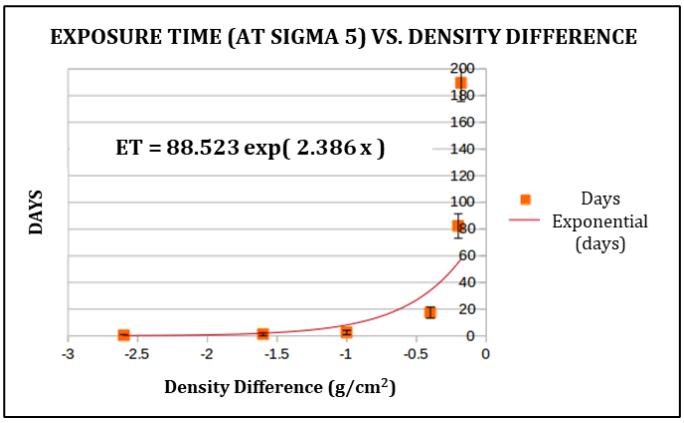

(d)

FIGURE 5: Some results from the simulations with the ore sphere geometry: (a) 1D and 2D histograms of the ratio using a sphere filled with air for an exposure time of just 1 day; (b) 1D and 2D histograms of the significance for the same conditions; (c) plot of ratio values as a function of density difference (R); (d) plot of exposure time for 5-sigma significance as a function of density difference (ET).

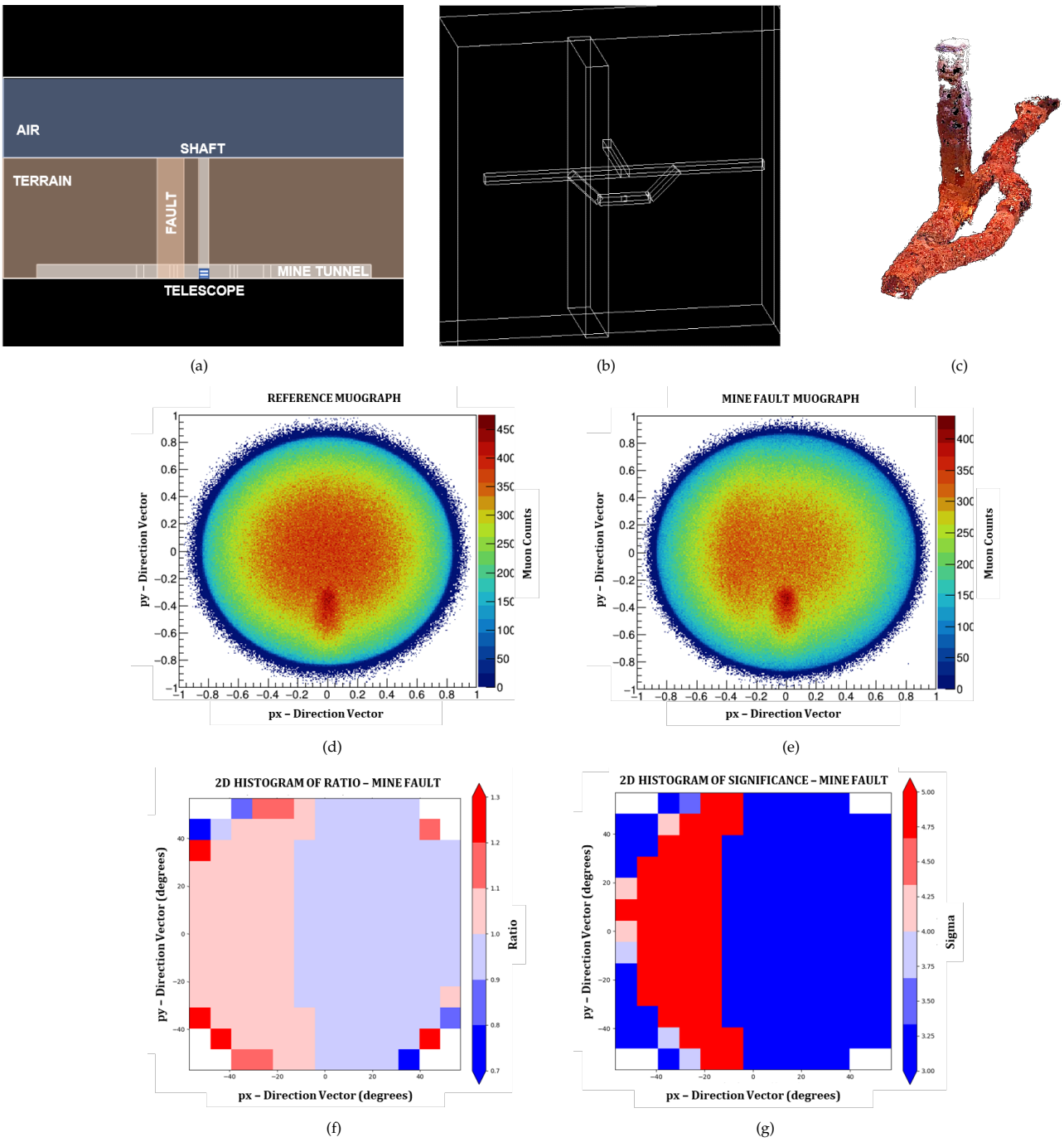

FIGURE 6: More realistic (than the first approach) geometry based on the section of the gallery where the prototype is located (near the Waldemar Shaft): (a) side view of the gallery section; (b) 3D bottom view of the geometry; (c) 3D Laser scan of the gallery section and Waldemar Shaft for reference; (d) reference muograph, with the shaft (darker red spot) and without the fault volume; axis values are the x and y components of the angular directional unit vector (4 days of exposure time); (e) muograph of the simulation with the shaft and the fault volume (4 days of exposure time); (f) 2D histogram of the ratio between the two muographs; the fault is visible in light red; (g) 2D histogram of the significance between the two muographs; the fault is visible in bright red.

ing some standard techniques. The mine gallery was mapped at a 1/2500 scale showing the different PQG and VSC rocks, VSC mineralization and their alteration near the surface by weathering. On this scale, the general volume distribution of the different mineralizations and rocks is used to guide the ground survey.

As initial steps for the surveys, a preliminary study of the application of the techniques was made through maps and on-site observations.

A sample of GPS coordinates was measured through differential GPS. Two Spectra EPOCH 50 GNSS Survey Systems antennas (Figure 7(a)) are used. One works as the base of the coordinates system, and another is coupled to a rover to accurately measure the coordinates of chosen targets (some naturally present, others artificially placed for completion). These coordinates are used for geopositioning the information gathered with photogrammetry and ground-based LIDAR.

A quadcopter drone DJI Phantom 4 Pro was used to photograph the surface above the mine (Figure 7(c)). The gathered information was treated with photogrammetry software, and the vegetation was then removed, to obtain a 3D digital elevation model, or DEM (Figure 7(d)), and a contour line DEM (Figure 7(e)). A detailed characterization of the topography is needed to separate the effect of distance and average density when analyzing the muon transmission results. The DEM can also be converted into a Geant4 geometry to use in the simulation; however, the computational feasibility of using a detailed geometry in large simulations is still under study.

To have a complete digital model with the surface and the gallery below, the scanning of the Waldemar Gallery is currently in the process with a ground-based LIDAR, model FARO Focus 3D Laser Scanner (Figure 7(b)). Auxiliary white sphere targets are placed on the ground for geopositioning, while the LIDAR does a 360° scan of the whole area around it. The scan is repeated throughout the interior of the gallery at spaced distances.

The photogrammetry and LIDAR information share some targets of geopositioning, so that both datasets can be merged in a single 3D digital model. In addition to being used in the geophysical analysis of muography, a photographic model like this can also be adapted for a virtual reality application to use in outreach activities in the science museum.

Two other geophysical methods are being used: the ground-penetrating radar (GPR) and the seismic refraction. At present, preliminary campaigns have tested the ground response so that the operational parameters of the equipment can be adjusted in future surveys for full coverage.

The GPR antennas emit electromagnetic pulses that penetrate the ground and receive the waves that were reflected in the interfaces of materials with different dielectric constants, measuring the amplitude and propagation time of the pulses.

In addition to the dielectric constant that controls the speed of the electromagnetic waves in the medium, the electrical resistivity of the ground controls the attenuation of the pulses and consequently the penetration distance until they extinguish. For the same frequency, the greater the conductivity, the greater the attenuation. Transversal profiles to the direction of the gallery are carried out in different locations with a GSSI SIR-3000 system using two antennas working in bistatic mode (separate transmitter-Tx and receiver-Rx antenna) and emitting pulses of the central frequency of 100 MHz (Figures 8(a) and 8(b)). The output information is given in GPR profiles with the ground materials in depth separated by their response to the electromagnetic pulses.

In the seismic refraction technique, a PASI Anteo multichannel exploration seismograph consisting of 48 geophones operating at 10 Hz is used (Figure 8(c)). The method of application is seismic refraction tomography, with the geophones positioned in profile and spaced 0.5 m apart. Geophones are the sensors that detect ground vibration waves (elastic longitudinal, or P waves), which in this case are produced with heavy hammer strokes on a metal plate (Figure 8(d)). The strokes are used as the source, and the metal plate is placed between the geophones, with repetition at regular intervals.

This technique measures, therefore, the propagation time of the vibration waves induced on the ground, in the path between the source and the geophones that capture the signal of the refracted waves. From these measurements, the velocity of the elastic waves through the various paths is calculated and, with that information, a 2D velocity model can be created.

The model shows the changes in the velocity propagation through the ground, giving knowledge about boundaries defined by changes in the geological parameters of the underground materials.

Rock samples were also collected in the proximity of the observation locations inside the gallery. Their physical parameters are now being analyzed. The density is the main parameter of interest, and humidity or electrical resistance might also prove useful. These direct measurements will provide reference values for all the other geophysical techniques, including muography.

6. WORK PROGRESSION AND FINAL CONSIDERATIONS

LouMu is a national project in which the muography technique is being developed independently. One of its strengths is the capacity and multidisciplinary nature of the team, which creates opportunities for education and outreach activities.

The geophysical and geological surveys are to be completed in advance of the muography observation. With all the information, a geological model is being created to use as the reference for the muography data analysis and the construction of more accurate simulations.

The muography analysis of the geology above the Lousal Mine is the focus of the current application of the technique. In this process, different tasks have to be accomplished, namely, the creation of simulations and muography analysis tools, the construction of a muon telescope and its calibration, which is currently under way, and on-site muon observations and information analysis. The result will be a reconstructed 3D density model of the region over the observation locations. The 3D density model will be evaluated to see how well the muography implementation was done and what adaptations can be made to improve the muon observations and the results. The muography survey in Lousal Mine is the first field application of the LouMu project, in which the foundations for other possible muography implementations are being developed.

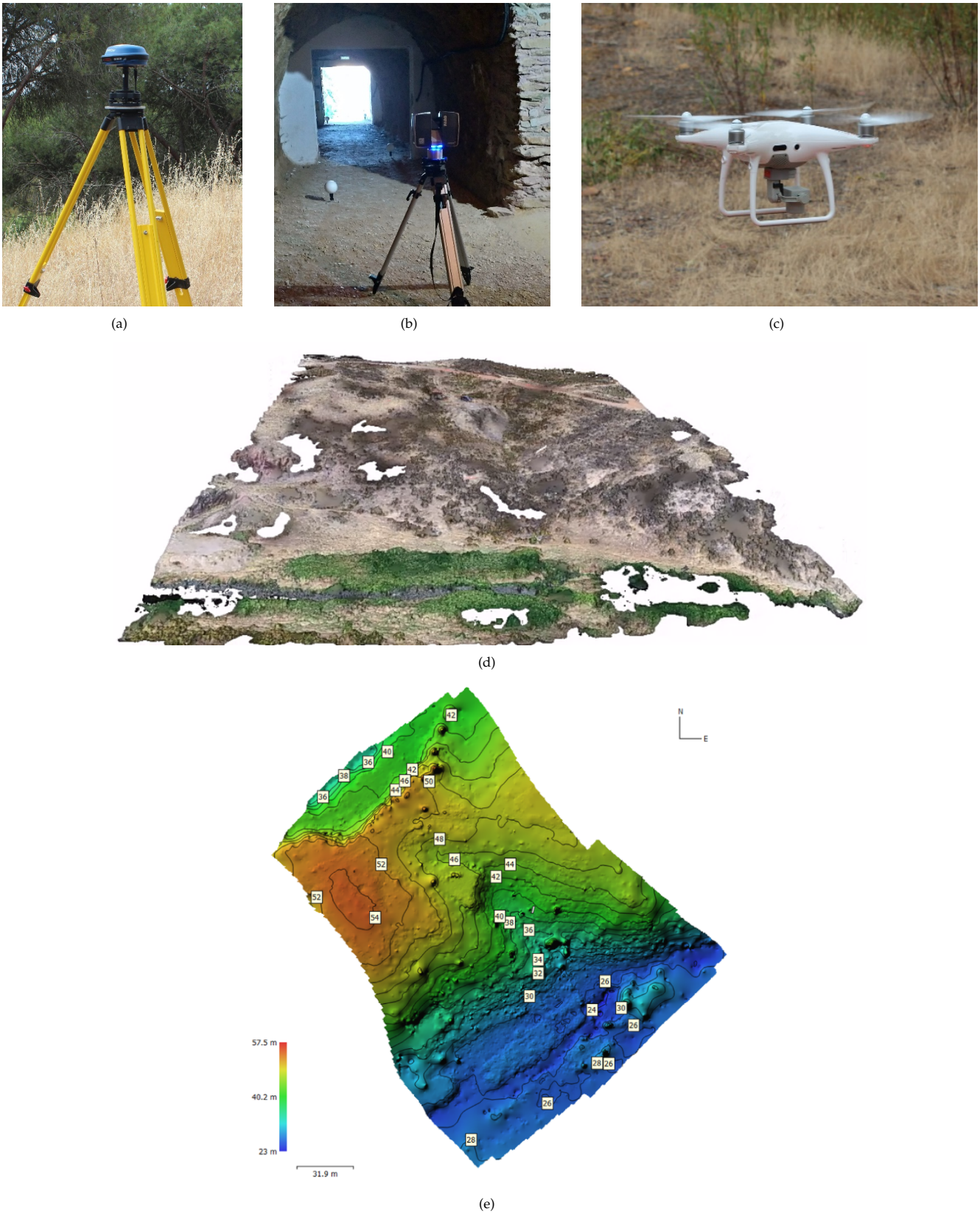

FIGURE 7: Differential GPS and photogrammetry equipment with results: (a) differential GPS antenna; (b) ground-based LIDAR; (c) photogrammetry aerial drone; (d) digital elevation model (DEM); (e) contour line DEM (altitude variation: 34.5 m).

FIGURE 8: (a) Two GPR antennas coupled together; (b) GPR measurements are done by moving the antennas in straight lines on the ground; (c) geophones that measure ground vibrations; (d) seismic signal induced with hammer strokes.

As outputs, this work is leading to adding geological information about the Lousal to the national geological heritage, to make available functional and stand-alone muon telescopes for the geophysical community and generalized muography methods to apply in other scenarios. In addition, throughout the project, outreach activities are conducted to educate local academics and the general public about muography. And in parallel, a multidisciplinary team is established with comprehensive knowledge and ability to share it to other communities.

CONFLICTS OF INTEREST

The authors declare that there are no conflicts of interest regarding the publication of this paper.

ACKNOWLEDGMENTS

This R&D project is financed by National Funds through the FCT - Foundation for Science and Technology, reference EXPL/FIS-OUT/1185/2021. The FCT also finances the Ph.D. scholarship, integrated into the LouMu, reference PD/BD/150490/2019, and within the scope of ICT, the project with reference UIDB/04683/2020. A grateful thanks go to the Lousal Ciência Viva team for their support of the project.

References

[1] S. Procureur, Muon imaging: principles, technologies and applications, Nucl. Inst. Methods A 878, 169 (2018). https://doi.org/10.1016/j.nima.2017.08.004.
[2] R. Kaiser, Muography: overview and future directions, Philos. Trans. R. Soc. A 377, 0049 (2018). https://doi.org/10.1098/rsta.2018.0049.
[3] L. Bonechi, R. D'Alessandro, A. Giammanco, Atmospheric muons as an imaging tool, Reviews in Physics, Volume 5, 100038, ISSN 2405-4283 (2020). https://doi.org/10.1016/j.revip.2020.100038.

[4] P. Teixeira et al., Muon Tomography applied in the Lousal Mine (Portugal), EGU2020-11834. https://doi.org/10.5194/egusphere-egu2020-11834.
[5] LouMu Webpage: https://pages.lip.pt/loumu/en/loumu/.
[6] S. Andringa et al., Muography in the University and in the Museum, Journal for Advanced Instrumentation in Science, vol. 2022, no. 1, Mar. 2022.
[7] J. M. R. S. Relvas, A. M. M. Pinto, J. X. Matos, Lousal, Portugal: a successful example of rehabilitation of a closed mine in the Iberian Pyrite Belt. Society for Geology Applied to Mineral Deposits SGA News, no. 31, June 2, 1–16 (2012).
[8] E. Ferreira da Silva et al., Mineralogy and geochemistry of trace metals and REE in volcanic massive sulfide host rocks, stream sediments, stream waters and acid mine drainage from the Lousal mine area (Iberian Pyrite Belt, Portugal). Applied Geochemistry, 24(3):383–401 (2009). https://doi.org/10.1016/j.apgeochem.2008.12.001.
[9] J. X. Matos et al., High resolution stratigraphy of the Phyllite-Quartzite Group in the northwest region of the Iberian Pyrite Belt, Portugal. Comunições Geológicas 101, Esp. I, 489-493, IX CNG/2° CoGePLiP, Porto, ISSN: 0873-948X, e-ISSN: 1647-581X (2014).
[10] J. Matos et al., Geophysical surveys in the Portuguese sector of the Iberian Pyrite Belt: a global overview focused on the massive sulphide exploration and geologic interpretation. Comunicações Geológicas. 107, 41–78 (2020).
[11] L. Lopes et al., Resistive Plate Chambers for the Pierre Auger array upgrade, Journal of Instrumentation 9 C10023 (2014). https://doi.org/10.1088/1748-0221/9/10/C10023.
[12] L. Lopes et al., Long term experience in Autonomous Stations and production quality control, Journal of Instrumentation 14 C07002 (2019). https://doi.org/10.1088/1748-0221/14/07/C07002.
[13] L. Lopes et al., Field Experience with Autonomous RPC Based Stations, Journal of Instrumentation 11 C09011 (2016). https://doi.org/10.1088/1748-0221/11/09/C09011.
[14] S. Agostinelli et al., GEANT4-a simulation toolkit, Nucl. Inst. Methods A 506, 250 (2003). https://doi.org/10.1016/S0168-9002(03)01368-8.
[15] N. Mori et al., A Geant4 framework for generic simulations of atmospheric muon detection experiments, Annals of Geophysics, 60 (2014). https://doi.org/10.4401/ag-7383.
[16] K. Nakamura and Particle Data Group, J. Phys. G: Nucl. Part. Phys. 37 075021 (2010). https://doi.org/10.1088/0954-3899/37/7A/075021.